Supporting information

Ligand and solvent control of selectivity in the C-H activation of a pyridylimine-substituted 1-naphthalene; a combined synthetic and computational study

Rena Simayi,[a] Simone M. Hansen,[b] Warren B. Cross,[b,*] Eric G. Hope,[a]
Kuldip Singh and Gregory A. Solan[a,*]

[a] Department of Chemistry, University of Leicester, University Road, Leicester LE1 7RH, UK
[b] School of Science and Technology, Nottingham Trent University, Clifton Lane, Nottingham NG11 8NS, UK

* Corresponding authors: gas8@leicester.ac.uk (G.A. Solan), warren.cross@ntu.ac.uk (W.B. Cross)

CONTENTS

PART A

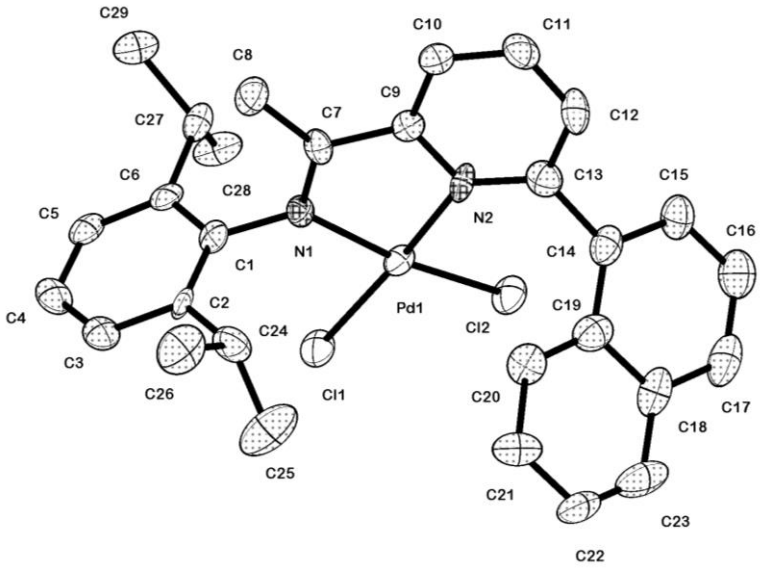

Figure S1 ORTEP representation of **1a** with thermal ellipsoids set at 50% probability level; all hydrogen atoms are omitted for clarity.

Table S1 Selected bond distances (Å) and angles (°) for **1a**

	Bond lengths
Pd(1)-N(2)	2.059(6)
Pd(1)-N(1)	2.010(6)
Pd(1)-Cl(2)	2.298(2)
Pd(1)-Cl(1)	2.270(2)
C(7)-N(1)	1.295(9)
C(13)-C(14)	1.518(11)
	Bond angles
N(2)-Pd(1)-Cl(2)	99.34(18)
N(2)-Pd(1)-Cl(1)	172.77(19)
N(2)-Pd(1)-N(1)	80.4(3)
N(1)-Pd(1)-Cl(2)	169.26(18)
N(1)-Pd(1)-Cl(1)	93.56(19)
Cl(1)-Pd(1)-Cl(2)	87.34(8)
C(7)-N(1)-C(1)	120.7(7)

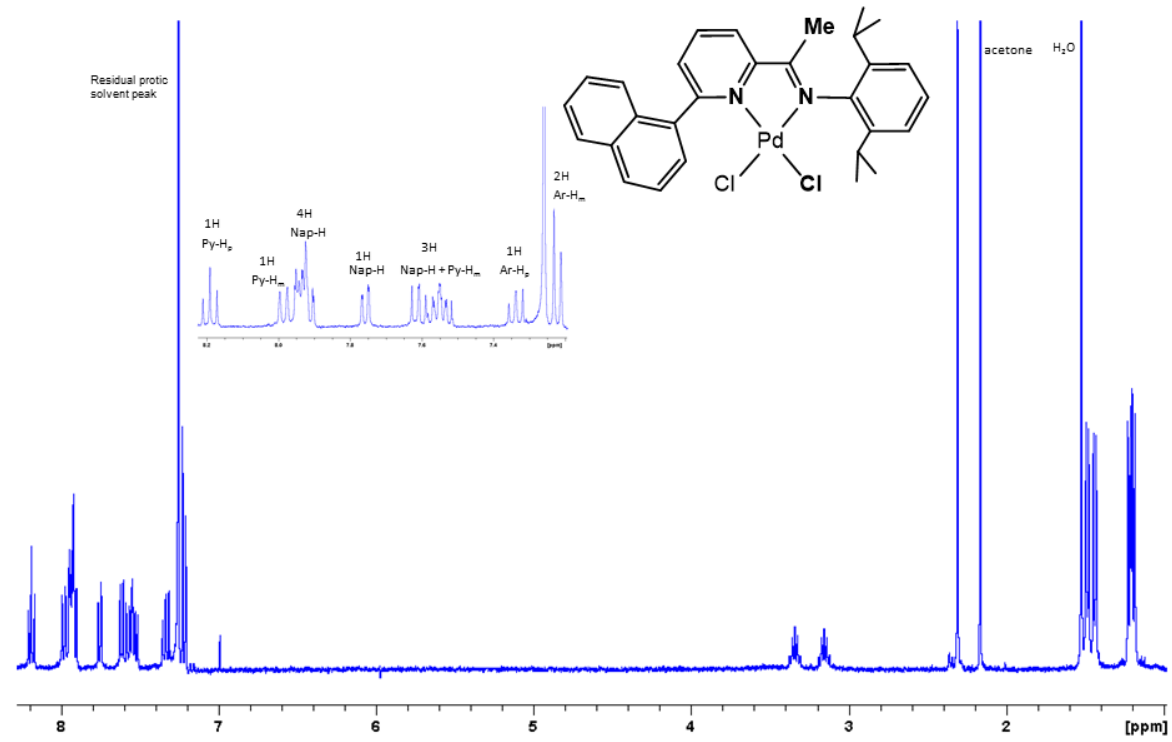

Figure S2 ^{1}H NMR spectrum of **1a** in $CDCl_3$ at room temperature

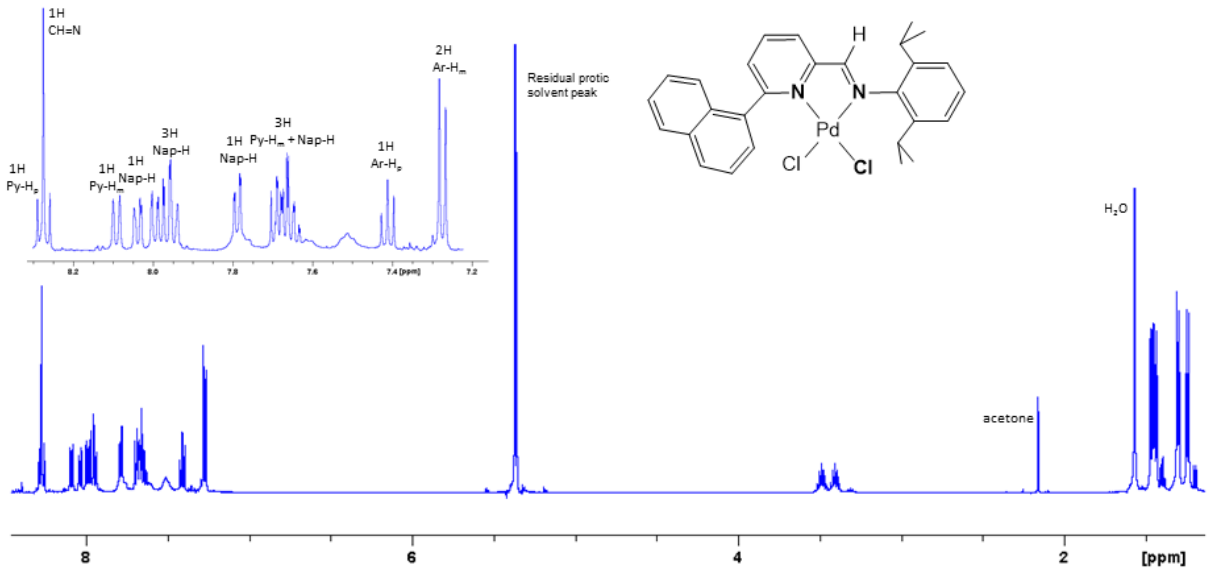

Figure S3 ^{1}H NMR spectrum of **1b** in CD_2Cl_2 at room temperature

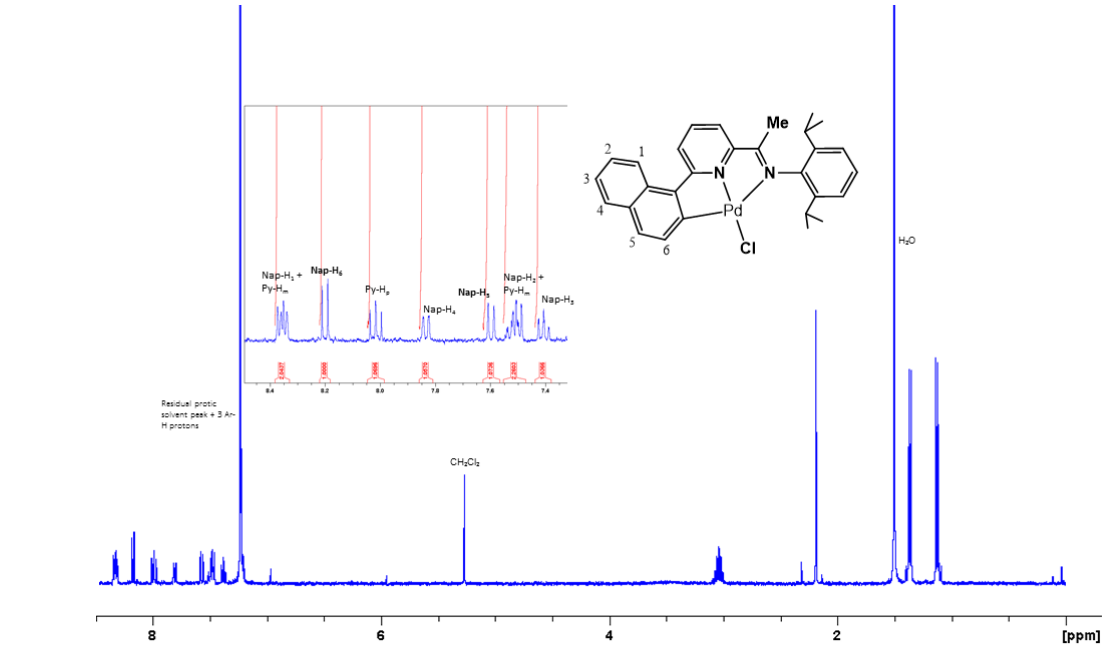

Figure S4a ^{1}H NMR spectrum of **2**$_{ortho}$ in $CDCl_3$ at room temperature

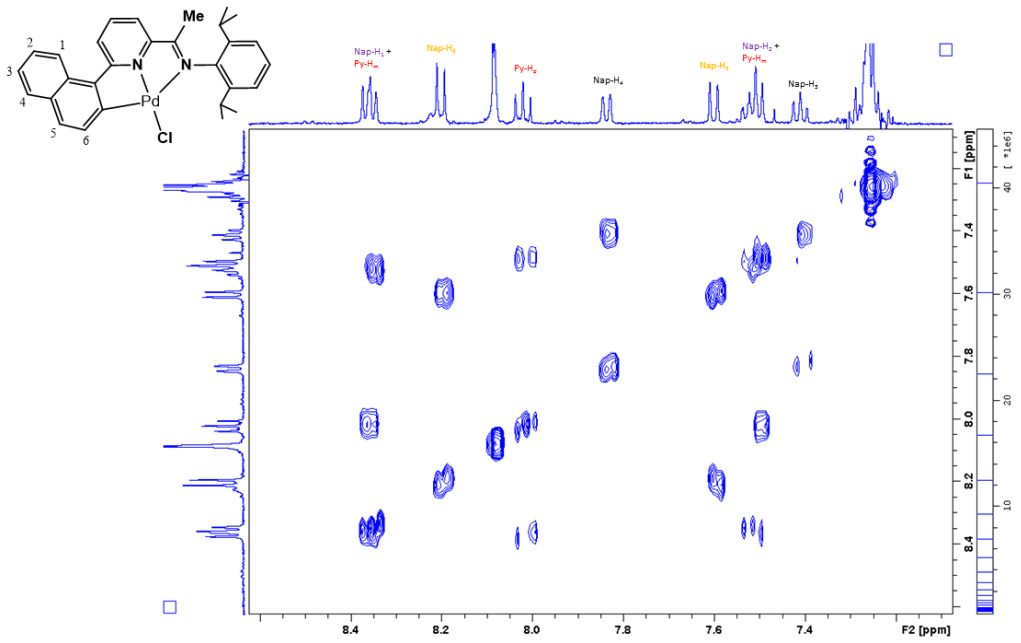

Figure S4b COSY spectrum of the aromatic region in **2**$_{ortho}$ in $CDCl_3$ at room temperature

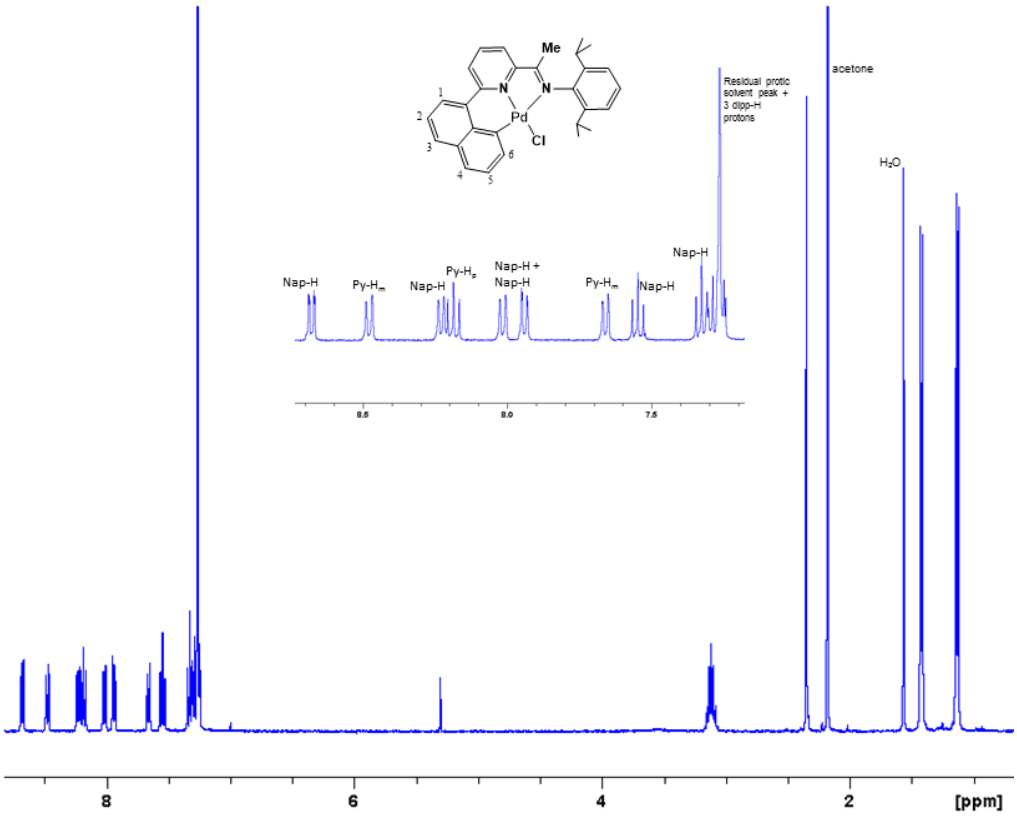

Figure S5a ^{1}H NMR spectrum of **2**$_{peri}$ in $CDCl_3$ at room temperature

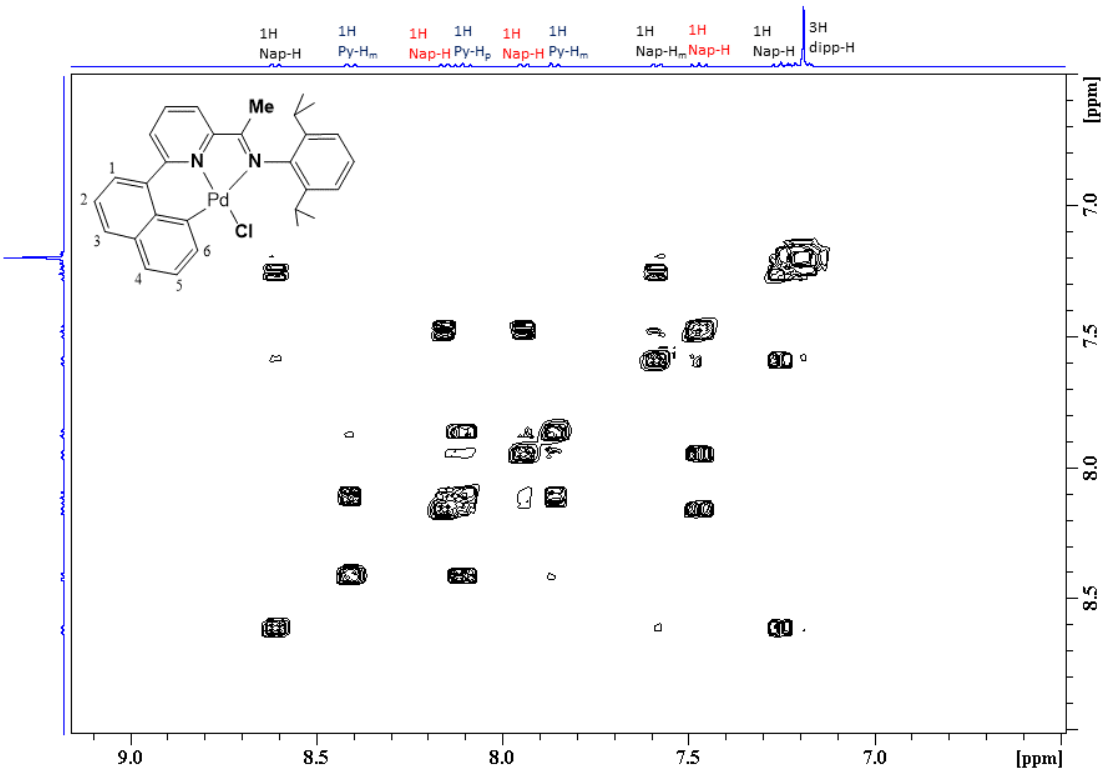

Figure S5b COSY spectrum of the aromatic region in **2**$_{peri}$ in $CDCl_3$ at room temperature

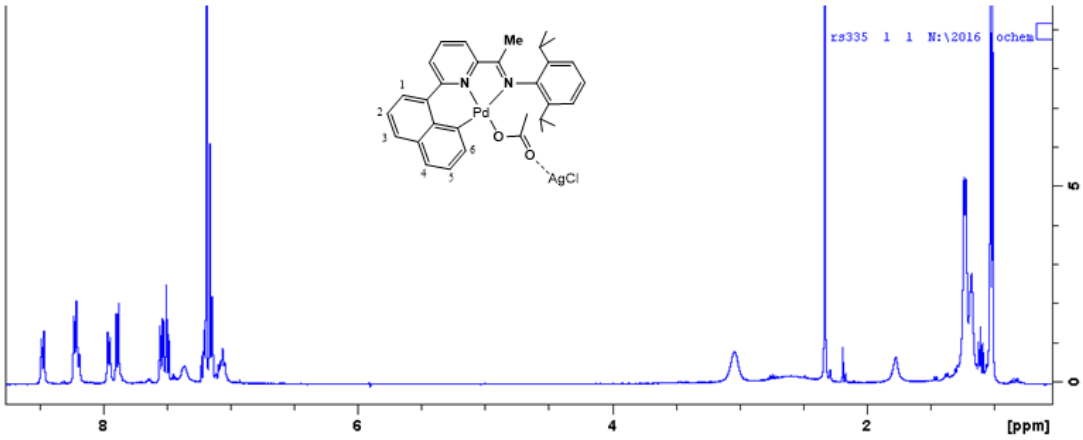

Figure S6 ^{1}H NMR spectrum of $\mathbf{3}_{\mathbf{peri}}\cdot$AgCl in $CDCl_3$ at room temperature

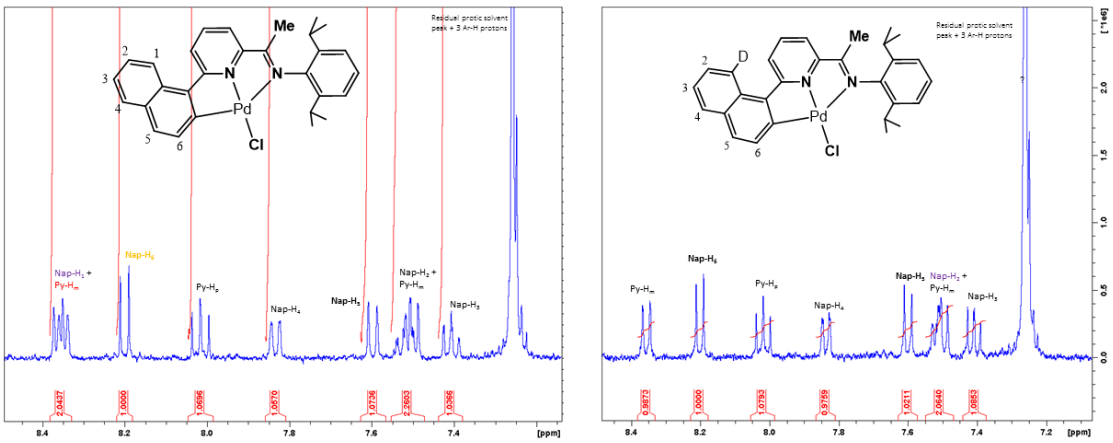

Figure S7 Side-by-side ^{1}H NMR spectra for $\mathbf{2}_{\text{ortho}}$ and *peri*-deuterated $\mathbf{2}_{\text{ortho}}$

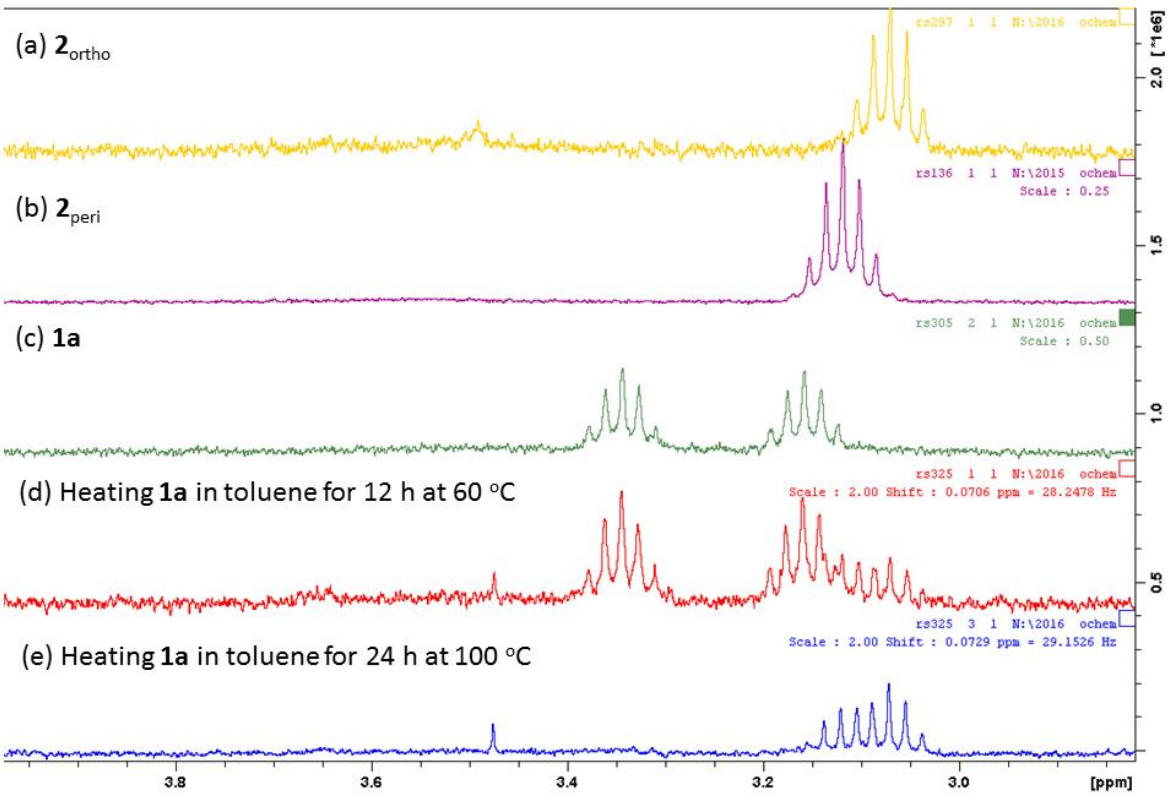

Figure S8 ^{1}H NMR spectra in the 2.8 – 4.0 ppm region of (a) $\mathbf{2}_{ortho}$, (b) $\mathbf{2}_{peri}$, (c) **1a**, (d) heating **1a** in toluene for 12 h at 60 °C, (e) heating **1a** in toluene for 24 h at 100 °C; all recorded in $CDCl_3$

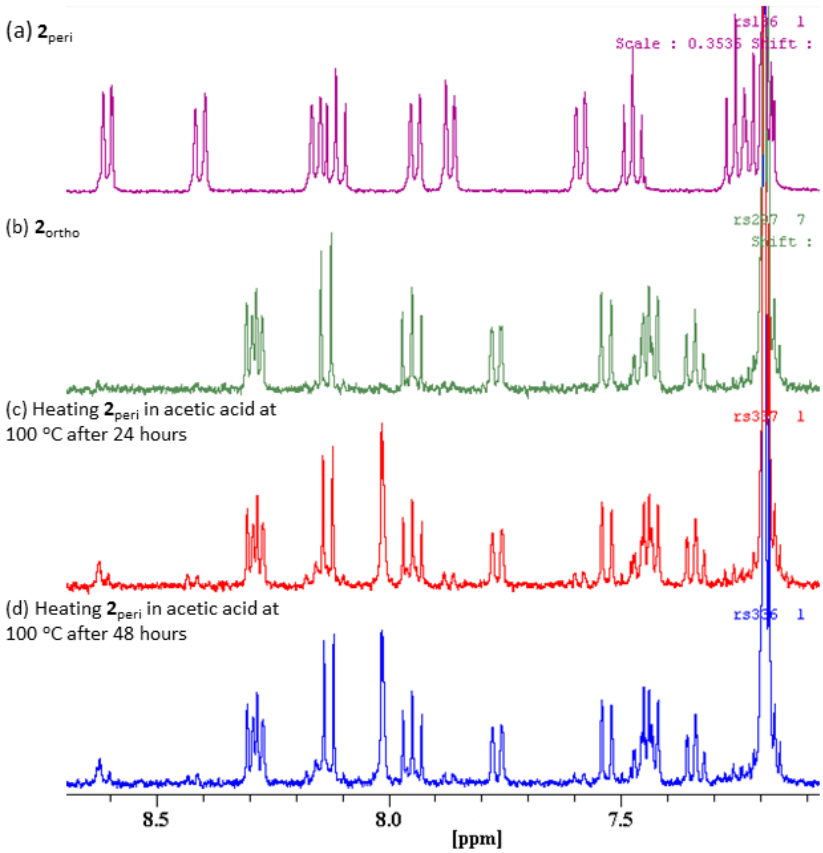

Figure S9 Aryl region of ^{1}H NMR spectra of (a) $\mathbf{2}_{peri}$, (b) $\mathbf{2}_{ortho}$, (c) after heating $\mathbf{2}_{peri}$ for 24 h at 100 °C in acetic acid and (d) after heating $\mathbf{2}_{ortho}$ at 100 °C for 48 h in acetic acid; all recorded in $CDCl_3$

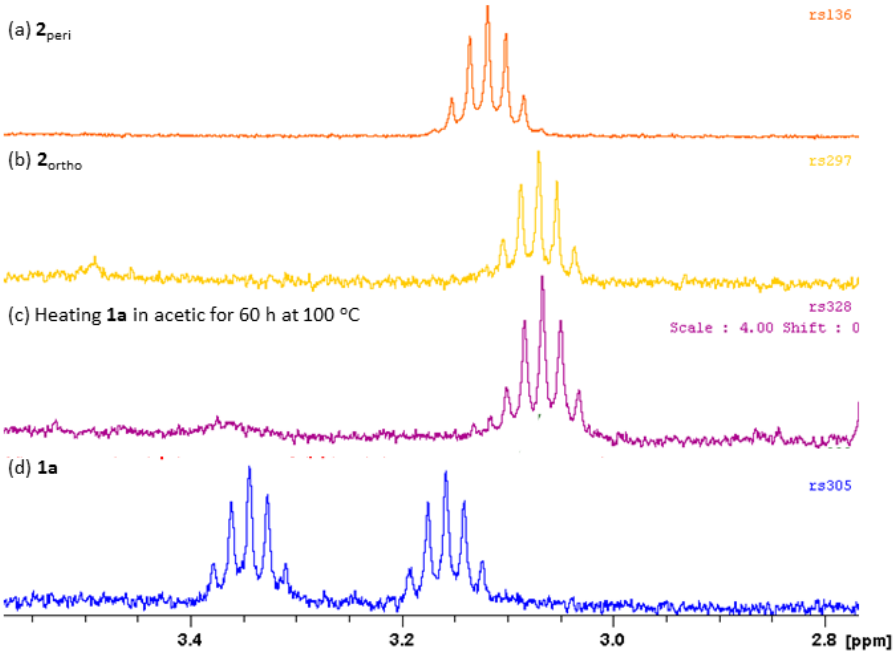

Figure S10 ^{1}H NMR spectra in the 2.8 – 4.0 ppm region of (a) $\mathbf{2}_{peri}$, (b) $\mathbf{2}_{ortho}$, (c) **1a**, (d) heating **1a** in acetic acid for 60 h at 100 °C, (e) **1a**; all recorded in $CDCl_3$ at room temperature

PART B

Computational Methods

Calculations were performed with Gaussian 09, Revision E.01.[S1] Geometry optimizations and thermal contributions to energies were computed in the gas phase with the gradient-corrected functional BP86[S2] and employed the SDD basis set for Pd with the Stuttgart/Dresden 28-electron ECP;[S3] the 6–31G(d,p) basis set was used for all other atoms.[S4] Stationary points were identified as minima or transition states through analytical frequency calculations; transition states were further characterised through IRC calculations and subsequent geometry optimisations. The energies reported in the main text are Gibbs energies that include both an empirical dispersion correction (Grimme's D3)[S5] and a solvent correction (AcOH or toluene, PCM approach).[S6]

Whereas C-H activation mediated by palladium carboxylate complexes has been thoroughly investigated by computational methods, C-H activation by palladium chloride complexes has been less well studied.[S7] Therefore all plausible mechanisms for the C-H activation of complex **1a** were investigated, including:

Fig. S11 and **Table S1**: concerted-metallation-deprotonation, involving an inner-sphere chloride ligand

Fig. S12 and **Table S2**: concerted-metallation-deprotonation, involving an outer-sphere chloride anion

Fig. S13 and **Table S3**: oxidative addition.

The concerted-metallation-deprotonation mechanism, involving an inner-sphere chloride ligand proved to be the lowest energy pathway; hence, this mechanism is the one presented in the main text.

A study testing the computational method was undertaken, see **Table S4**.

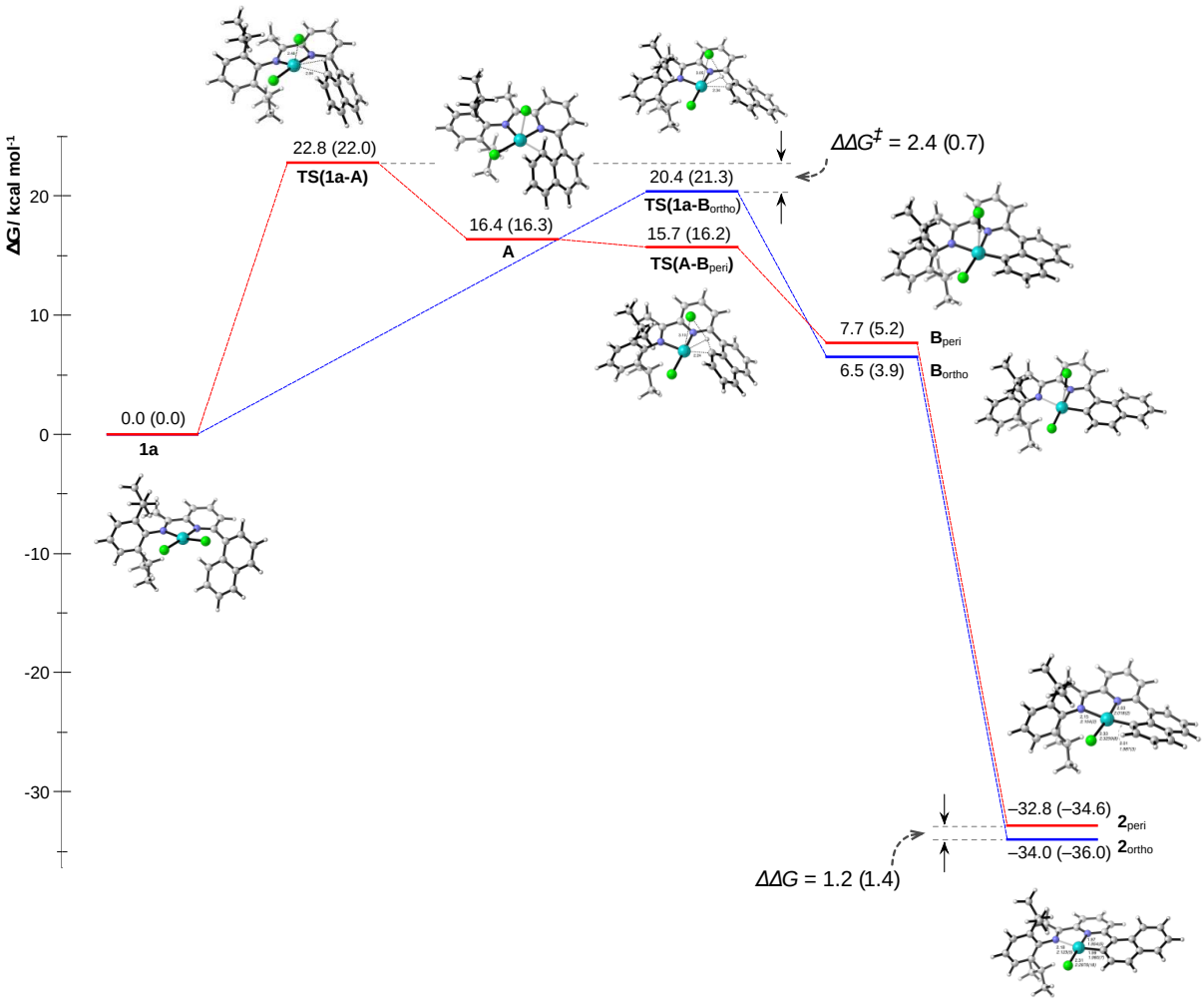

Figure S11. Computed reaction profile for the C-H activation of **1a** *via* an **inner-sphere concerted-metallation-deprotonation mechanism**. Energies were calculated at the BP86+D3/SDD/6-31G(d,p) level and include a PCM solvent correction in acetic acid or toluene (parentheses).

Table S1. Computed relative energies for the C-H activation of **1a** *via* an **inner-sphere concerted-metallation-deprotonation mechanism**. Energies were calculated at the BP86+D3/SDD/6-31G(d,p) level and include a PCM solvent correction. Data in bold are those used in the main text.

	Solvent = AcOH					**Solvent = PhMe**				
	SCF energy	**SCF + ZP energy**	**SCF + thermal energy**	**SCF + thermal enthalpy**	**SCF + thermal free energy**	**SCF energy**	**SCF + ZP energy**	**SCF + thermal energy**	**SCF + thermal enthalpy**	**SCF + thermal free energy**
1a	0.0	0.0	0.0	0.0	0.0	0.0	0.0	0.0	0.0	**0.0**
TS(1a-A)	22.3	21.8	21.4	21.4	**22.8**	21.5	21.0	20.6	20.6	**22.0**
A	16.2	15.6	15.7	15.7	**16.4**	16.1	15.5	15.6	15.6	**16.3**
TS(A-B$_{peri}$)	15.2	14.1	13.7	13.7	**15.7**	15.6	14.6	14.2	14.2	**16.2**
TS(1a-B$_{ortho}$)	21.7	20.1	19.9	19.9	**20.4**	22.6	21.0	20.8	20.8	**21.3**
B$_{ortho}$	10.4	7.5	7.8	7.8	**6.5**	7.8	5.0	5.3	5.3	**3.9**
B$_{peri}$	10.1	7.5	7.6	7.6	**7.7**	7.6	5.0	5.1	5.1	**5.2**
2$_{ortho}$ + HCl	21.3	17.5	39.1	40.3	**-34.0**	19.3	15.5	37.1	38.3	**-36.0**
2$_{peri}$ + HCl	21.9	18.2	39.7	40.9	**-32.8**	20.0	16.4	37.8	39.0	**-34.6**

** in the gas phase, **A** is lower in energy than **TS(A-B$_{peri}$)**, including with the dispersion correction; when the solvent correction is applied, A is higher in energy than **TS(A-B$_{peri}$)**.*

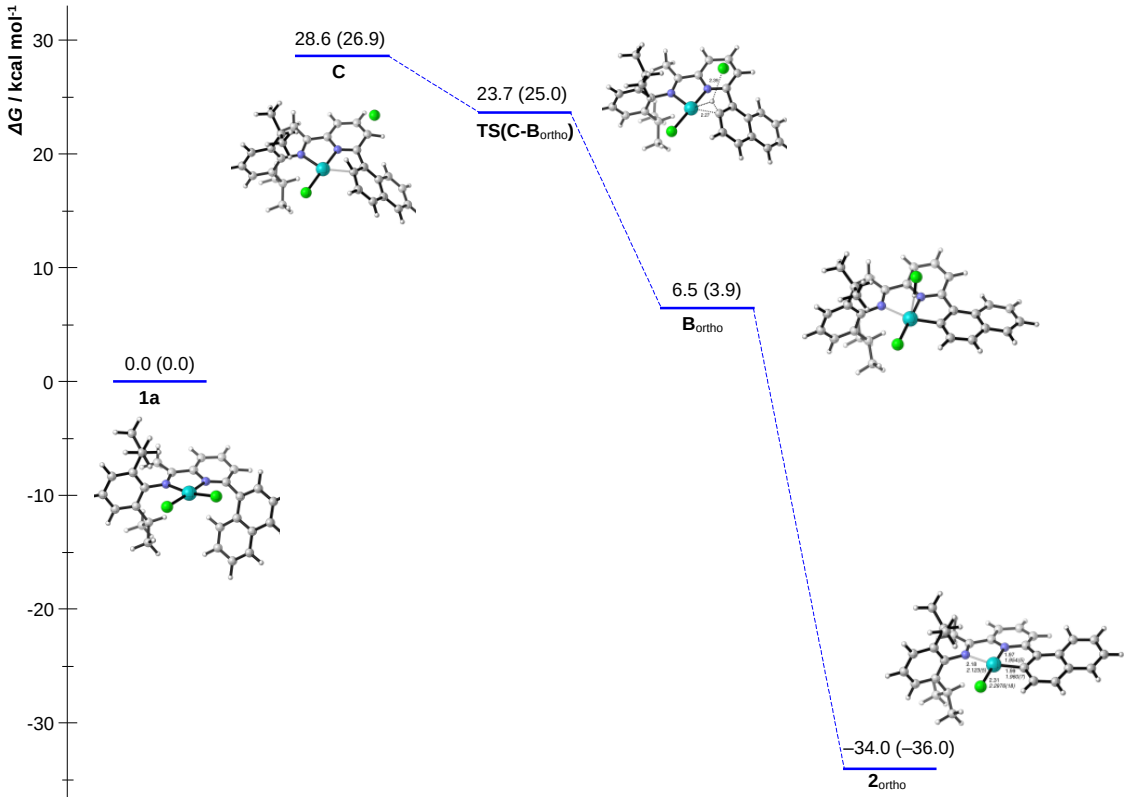

Figure S12. Computed reaction profile for the C-H activation of **1a** *via* an **outer-sphere concerted-metallation-deprotonation mechanism**. A pathway for the *ortho*-C-H activation only could be located. Energies were calculated at the BP86+D3/SDD/6-31G(d,p) level and include a PCM solvent correction for acetic acid or toluene (parentheses).

Table S2. Computed relative energies for the C-H activation of **1a** *via* an **outer-sphere concerted-metallation-deprotonation mechanism**. Energies were calculated at the BP86+D3/SDD/6-31G(d,p) level and include a PCM solvent correction.

	Solvent = AcOH					**Solvent = PhMe**				
	SCF energy	**SCF + ZP energy**	**SCF + thermal energy**	**SCF + thermal enthalpy**	**SCF + thermal free energy**	**SCF energy**	**SCF + ZP energy**	**SCF + thermal energy**	**SCF + thermal enthalpy**	**SCF + thermal free energy**
1a	0.0	0.0	0.0	0.0	**0.0**	0.0	0.0	0.0	0.0	**0.0**
C	30.1	29.3	29.6	29.6	**28.6**	28.3	27.6	27.8	27.8	**26.9**
TS(C-B$_{ortho}$)	24.7	23.5	23.2	23.2	**23.7**	26.0	24.7	24.5	24.5	**25.0**
B$_{ortho}$	10.4	7.5	7.8	7.8	**6.5**	7.8	5.0	5.3	5.3	**3.9**
2$_{ortho}$ + HCl	21.3	17.5	39.1	40.3	**-34.0**	19.3	15.5	37.1	38.3	**-36.0**

** in the gas phase, **C** is lower in energy than **TS(C-B$_{ortho}$)**, including with the dispersion correction; when the solvent correction is applied, C is higher in energy than **TS(C-B$_{ortho}$)**.*

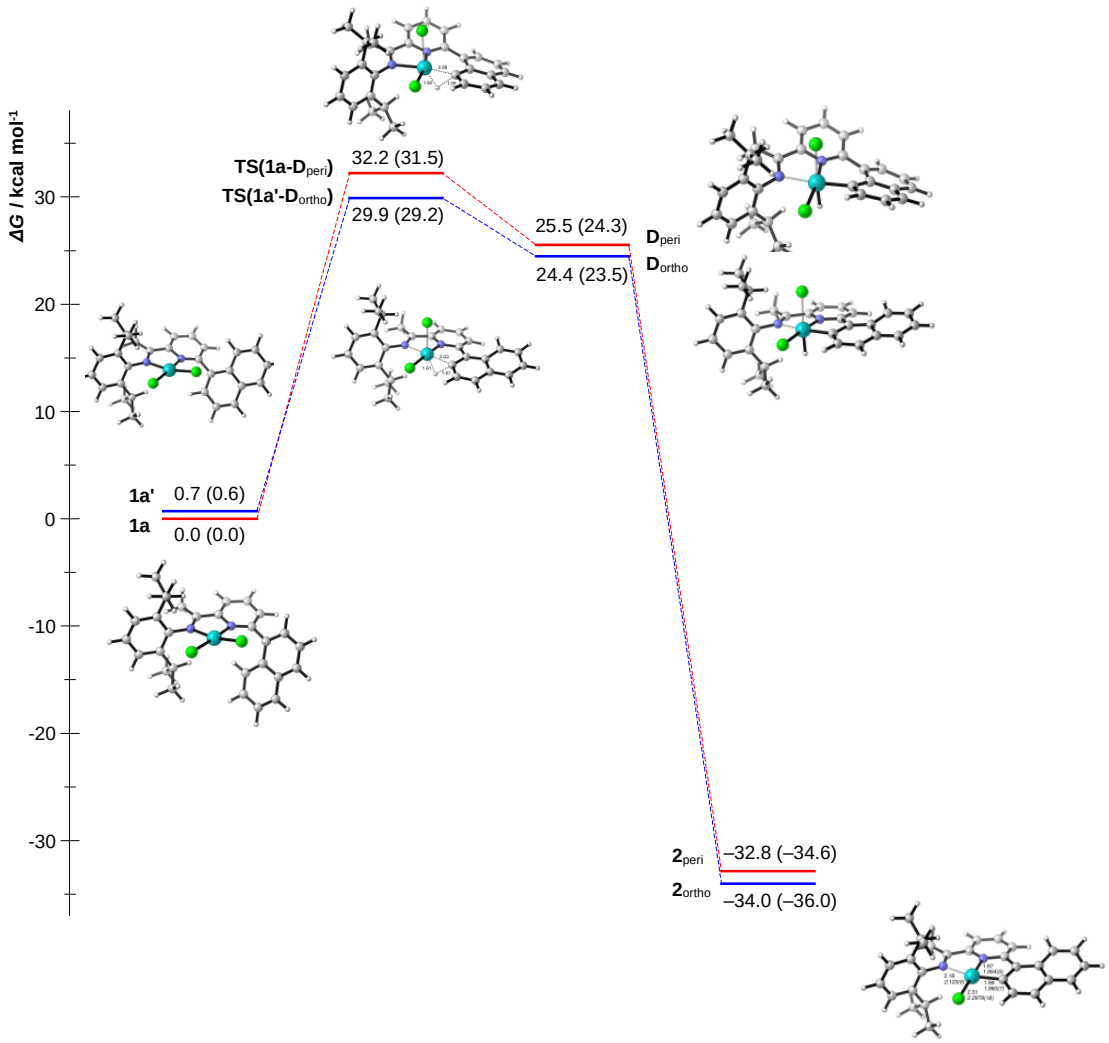

Figure S13. Computed reaction profile for the C-H activation of **1a** *via* an **oxidative addition mechanism**. Energies were calculated at the BP86+D3/SDD/6-31G(d,p) level and include a PCM solvent correction for acetic acid or toluene (parentheses).

Table S3. Computed relative energies for the C-H activation of **1a** *via* an **oxidative addition mechanism**. Energies were calculated at the BP86+D3/SDD/6-31G(d,p) level and include a PCM solvent correction.

	Solvent = AcOH					**Solvent = PhMe**				
	SCF energy	**SCF + ZP energy**	**SCF + thermal energy**	**SCF + thermal enthalpy**	**SCF + thermal free energy**	**SCF energy**	**SCF + ZP energy**	**SCF + thermal energy**	**SCF + thermal enthalpy**	**SCF + thermal free energy**
1a	0.0	0.0	0.0	0.0	**0.0**	0.0	0.0	0.0	0.0	**0.0**
1a'	0.7	0.7	0.7	0.7	**0.7**	0.6	0.6	0.6	0.6	**0.6**
TS(1a'-D_{ortho})	32.1	29.0	28.8	28.8	**29.9**	31.5	28.3	28.1	28.1	**29.2**
TS(1a-D_{peri})	33.8	30.7	30.4	30.4	**32.2**	33.1	30.1	29.7	29.7	**31.5**
D_{ortho}	25.4	23.5	23.4	23.4	**24.4**	24.4	22.6	22.5	22.5	**23.5**
D_{peri}	25.5	23.7	23.5	23.5	**25.5**	24.3	22.6	22.3	22.3	**24.3**
2_{ortho} + HCl	21.3	17.5	39.1	40.3	**-34.0**	19.3	15.5	37.1	38.3	**-36.0**
2_{peri} + HCl	21.9	18.2	39.7	40.9	**-32.8**	20.0	16.4	37.8	39.0	**-34.6**

Table S4. Method testing: relative computed energies for the C-H activation of **1a**; energies are Gibbs free energies in kcal/mol.

Single-point calculations at the *M06/def2-TZVP//BP86/SDD/6-31G(d,p) + D3 + solvent* level broadly show the same trends as the *BP86/SDD/6- 31G(d,p) + D3 + solvent* calculations reported in the main text; however, the former calculations gave higher energy transition state energies that are inconsistent with the experimental conditions under which the reactions were conducted.

Inner-sphere CMD mechanism

	1a	TS(1a-A)	A	TS(A-B:peri)	TS(1a-B:ortho)	B:ortho	B:peri	2:ortho + HCl	2:peri + HCl
BP86/SDD/6-31G(d,p)	0	21.3	19.0	19.9	22.4	-0.8	2.7	-47.4	-44.0
BP86/SDD/6-31G(d,p) + D3	0	21.4	16.5	17.5	23.0	1.2	2.5	-38.1	-36.6
M06/def2-TZVP//BP86/SDD/6-31G(d,p)	0	26.2	22.3	21.8	28.6	7.9	9.6	-36.3	-34.9
M06/def2-TZVP//BP86/SDD/6-31G(d,p) + D3	0	26.4	22.3	21.8	29.0	8.2	9.5	-34.5	-33.3
BP86/SDD/6-31G(d,p) + D3 + AcOH	**0**	**22.8**	**16.4**	**15.7**	**20.4**	**6.5**	**7.7**	**-34.0**	**-32.8**
M06/def2-TZVP//BP86/SDD/6-31G(d,p) + D3 + AcOH	0	27.8	21.1	19.3	25.2	14.2	15.5	-29.5	-29.2
BP86/SDD/6-31G(d,p) + D3 + PhMe	**0**	**22.0**	**16.3**	**16.2**	**21.3**	**3.9**	**5.2**	**-36.0**	**-34.6**
M06/def2-TZVP//BP86/SDD/6-31G(d,p) + D3 + PhMe	0	27.0	21.4	20.0	26.5	11.3	12.7	-24.4	-23.3

Outer-sphere CMD mechanism

	1a	C	TS(C-B:ortho)	B:ortho	2:ortho + HCl
BP86/SDD/6-31G(d,p)	0	22.4	26.4	-0.8	-47.4
BP86/SDD/6-31G(d,p) + D3	0	25.8	27.6	1.2	-38.1
M06/def2-TZVP//BP86/SDD/6-31G(d,p)	0	33.1	33.0	7.9	-36.3
M06/def2-TZVP//BP86/SDD/6-31G(d,p) + D3	0	33.8	33.5	8.2	-34.5
BP86/SDD/6-31G(d,p) + D3 + AcOH	**0**	**28.6**	**23.7**	**6.5**	**-34.0**
M06/def2-TZVP//BP86/SDD/6-31G(d,p) + D3 + AcOH	0	37.1	28.4	14.2	-29.5
BP86/SDD/6-31G(d,p) + D3 + PhMe	**0**	**26.9**	**25.0**	**3.9**	**-36.0**
M06/def2-TZVP//BP86/SDD/6-31G(d,p) + D3 + PhMe	0	35.2	30.1	11.3	-24.4

Table S4 continued. Method testing: relative computed energies for the C-H activation of **1a**; energies are Gibbs free energies in kcal/mol.

Oxidative addition mechanism

	1a	1a'	TS(1a'-D:ortho)	TS(1a-D:peri)	D:ortho	D:peri	2:ortho + HCl	2:peri + HCl
BP86/SDD/6-31G(d,p)	0	-1.3	27.7	32.5	22.1	25.3	-47.4	-44.0
BP86/SDD/6-31G(d,p) + D3	0	0.7	28.6	30.9	22.7	23.2	-38.1	-36.6
M06/def2-TZVP//BP86/SDD/6-31G(d,p)	0	0.2	41.4	44.7	39.7	40.7	-36.3	-34.9
M06/def2-TZVP//BP86/SDD/6-31G(d,p) + D3	0	0.8	41.9	44.8	40.1	40.7	-34.5	-33.3
BP86/SDD/6-31G(d,p) + D3 + AcOH	**0**	**0.7**	**29.9**	**32.2**	**24.4**	**25.5**	**-34.0**	**-32.8**
M06/def2-TZVP//BP86/SDD/6-31G(d,p) + D3 + AcOH	0	0.9	43.6	46.3	42.6	43.8	-29.5	-29.2
BP86/SDD/6-31G(d,p) + D3 + PhMe	**0**	**0.6**	**29.2**	**31.5**	**23.5**	**24.3**	**-36.0**	**-34.6**
M06/def2-TZVP//BP86/SDD/6-31G(d,p) + D3 + PhMe	0	0.8	42.7	45.5	41.3	42.3	-24.4	-23.3

Computed Structures and energies (hartrees) for all species computed

Cartesian coordinates are placed in a separate text file for convenient visualization

1a, (HL:Me)$PdCl_2$

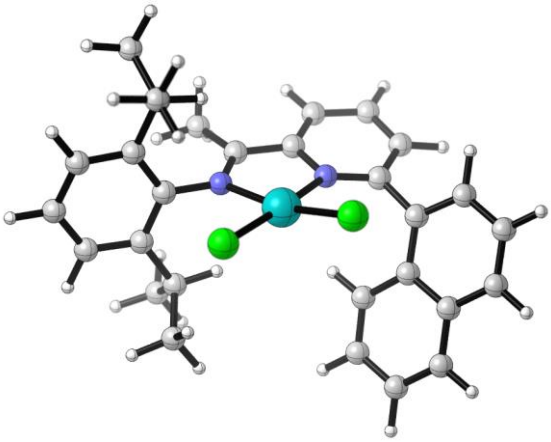

SCF Energy (gas phase)= -2281.22921882
Zero-point correction= 0.505339 (Hartree/Particle)
Thermal correction to Energy = 0.539722
Thermal correction to Enthalpy = 0.540666
Thermal correction to Gibbs Free Energy = 0.438184
SCF Energy (AcOH + D3) = -2281.36140360
SCF Energy (PhMe + D3) = -2281.34989147

1a', (HL:Me)PdCl2

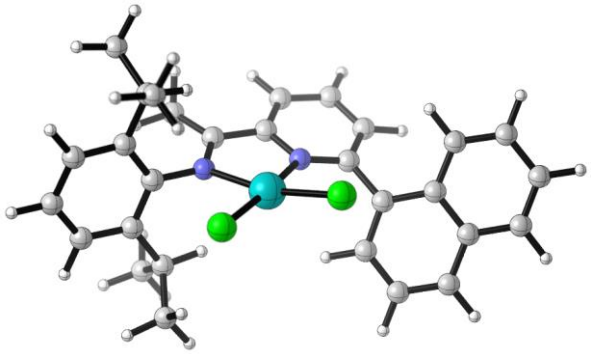

SCF Energy (gas phase) = -2281.23141176
Zero-point correction= 0.505412 (Hartree/Particle)
Thermal correction to Energy = 0.539756
Thermal correction to Enthalpy = 0.540700
Thermal correction to Gibbs Free Energy = 0.438249
SCF Energy (AcOH + D3) = -2281.36030137
SCF Energy (PhMe + D3) = -2281.34896433

2:ortho, (L:Me)PdCl

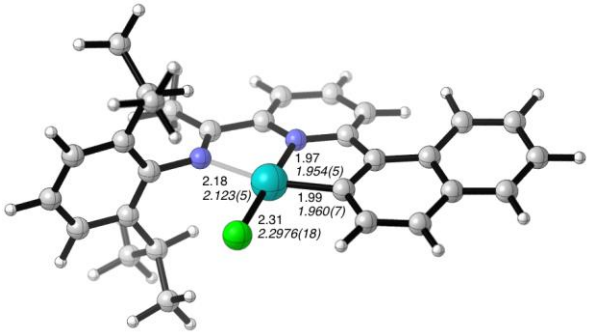

SCF Energy (gas phase) = -1820.38825239
Zero-point correction= 0.492810 (Hartree/Particle)
Thermal correction to Energy = 0.524871
Thermal correction to Enthalpy = 0.525815
Thermal correction to Gibbs Free Energy = 0.428620
SCF Energy (AcOH + D3) = -1820.49625972
SCF Energy (PhMe + D3) = -1820.48910619

2:peri, (L:Me)PdCl

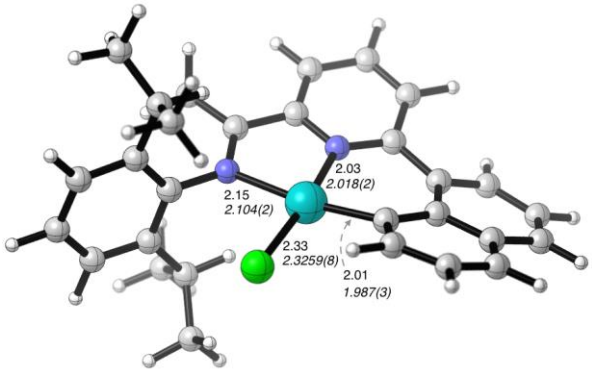

SCF Energy (gas phase) = -1820.38380958
Zero-point correction= 0.492961 (Hartree/Particle)
Thermal correction to Energy = 0.524826
Thermal correction to Enthalpy = 0.525770
Thermal correction to Gibbs Free Energy = 0.429626
SCF Energy (AcOH + D3) = -1820.49536187
SCF Energy (PhMe + D3) = -1820.48790615

TS(1a-A)

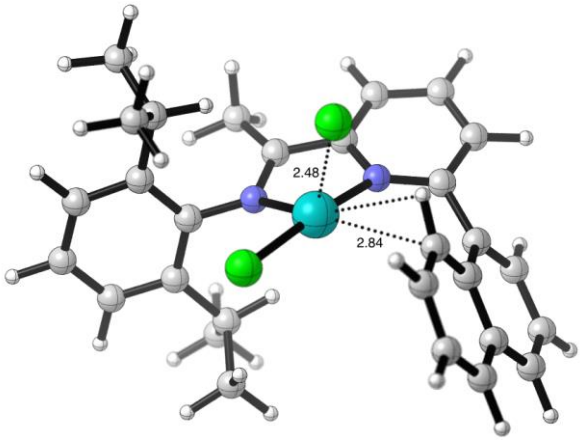

SCF Energy (gas phase) = -2281.19599490
Zero-point correction= 0.504469 (Hartree/Particle)
Thermal correction to Energy = 0.538216
Thermal correction to Enthalpy = 0.539160
Thermal correction to Gibbs Free Energy = 0.438966
Lowest frequency = -36.80cm-1
SCF Energy (AcOH + D3) = -2281.32581907
SCF Energy (PhMe + D3) = -2281.31555391

A, (HL:Me)PdCl2

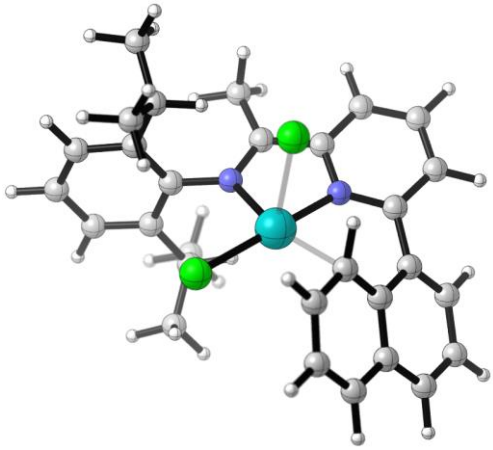

SCF Energy (gas phase) = -2281.19916670
Zero-point correction= 0.504372 (Hartree/Particle)
Thermal correction to Energy = 0.538908
Thermal correction to Enthalpy = 0.539852
Thermal correction to Gibbs Free Energy = 0.438454
SCF Energy (AcOH + D3) = -2281.33556815
SCF Energy (PhMe + D3) = -2281.32422110

TS(1a-B:ortho)

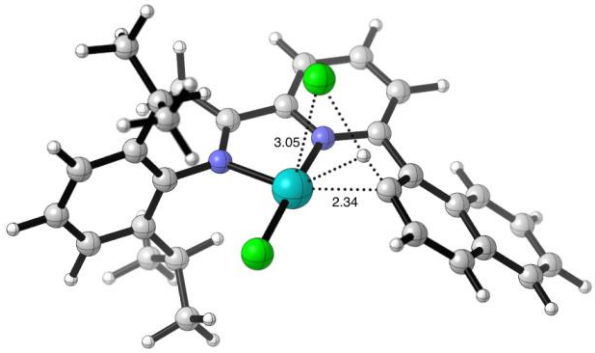

SCF Energy (gas phase) = -2281.19138151
Zero-point correction= 0.502811 (Hartree/Particle)
Thermal correction to Energy = 0.536871
Thermal correction to Enthalpy = 0.537816
Thermal correction to Gibbs Free Energy = 0.436125
Lowest frequency = -52.23cm-1
SCF Energy (AcOH + D3) = -2281.32686823
SCF Energy (PhMe + D3) = -2281.31387283

TS(A-B:peri)

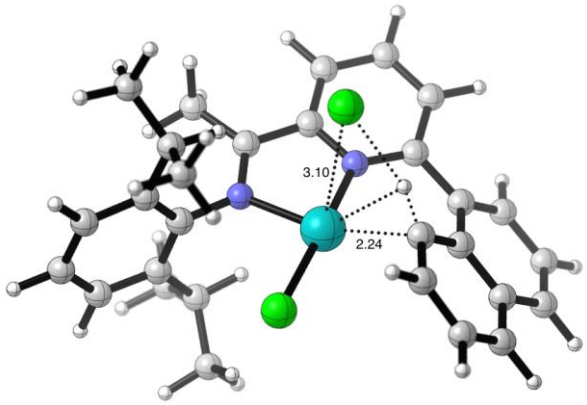

SCF Energy (gas phase) = -2281.19839780
Zero-point correction= 0.503726 (Hartree/Particle)
Thermal correction to Energy = 0.537422
Thermal correction to Enthalpy = 0.538367
Thermal correction to Gibbs Free Energy = 0.439000
Lowest frequency = -29.77cm-1
SCF Energy (AcOH + D3) = -2281.33724852
SCF Energy (PhMe + D3) = -2281.32496324

B:ortho, (L:Me)PdCl(HCl)

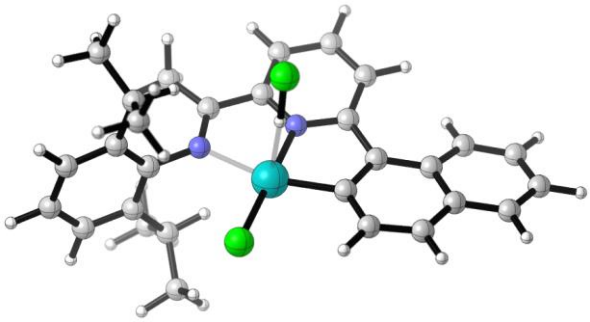

SCF Energy (gas phase) = -2281.22434427
Zero-point correction= 0.500819 (Hartree/Particle)
Thermal correction to Energy = 0.535718
Thermal correction to Enthalpy = 0.536662
Thermal correction to Gibbs Free Energy = 0.431977
SCF Energy (AcOH + D3) = -2281.34490745
SCF Energy (PhMe + D3) = -2281.33743048

B:peri, (L:Me)PdCl(HCl)

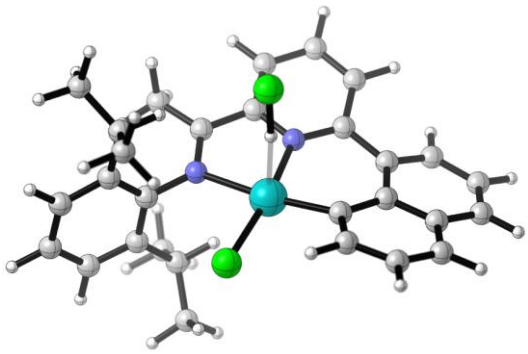

SCF Energy (gas phase) = -2281.22103219
Zero-point correction= 0.501147 (Hartree/Particle)
Thermal correction to Energy = 0.535706
Thermal correction to Enthalpy = 0.536651
Thermal correction to Gibbs Free Energy = 0.434295
SCF Energy (AcOH + D3) = -2281.34530822
SCF Energy (PhMe + D3) = -2281.33771636

C, [(HL:Me)PdCl][Cl]

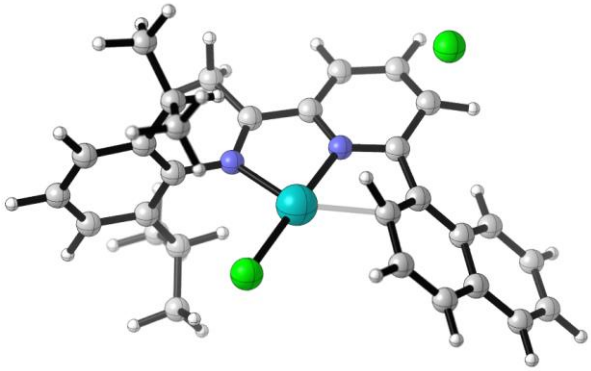

SCF Energy (gas phase) = -2281.19117861
Zero-point correction= 0.504116 (Hartree/Particle)
Thermal correction to Energy = 0.538934
Thermal correction to Enthalpy = 0.539878
Thermal correction to Gibbs Free Energy = 0.435827
SCF Energy (AcOH + D3) = -2281.31349099
SCF Energy (PhMe + D3) = -2281.30474228

TS(C-B:ortho)

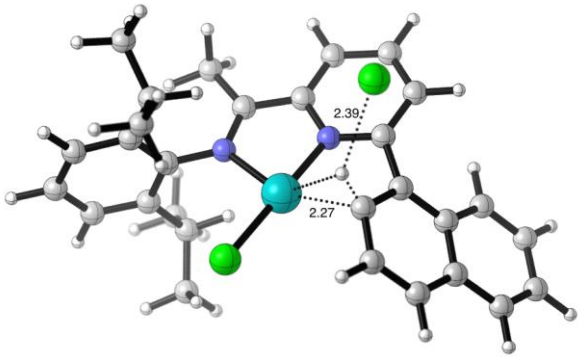

SCF Energy (gas phase) = -2281.18540575
Zero-point correction= 0.503283 (Hartree/Particle)
Thermal correction to Energy = 0.537331
Thermal correction to Enthalpy = 0.538276
Thermal correction to Gibbs Free Energy = 0.436493
Lowest frequency = -70.62cm-1
SCF Energy (AcOH + D3) = -2281.32196944
SCF Energy (PhMe + D3) = -2281.30842954

TS(1a'-D:ortho)

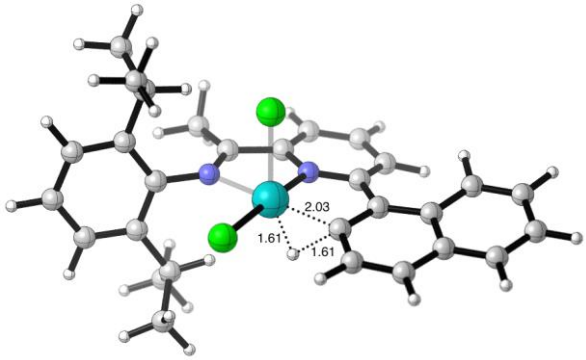

SCF Energy (gas phase) = -2281.18153450
Zero-point correction= 0.500317 (Hartree/Particle)
Thermal correction to Energy = 0.534327
Thermal correction to Enthalpy = 0.535271
Thermal correction to Gibbs Free Energy = 0.434625
Lowest frequency = -809.35cm-1
SCF Energy (AcOH + D3) = -2281.31017101
SCF Energy (PhMe + D3) = -2281.29976042

TS(1a-D:peri)

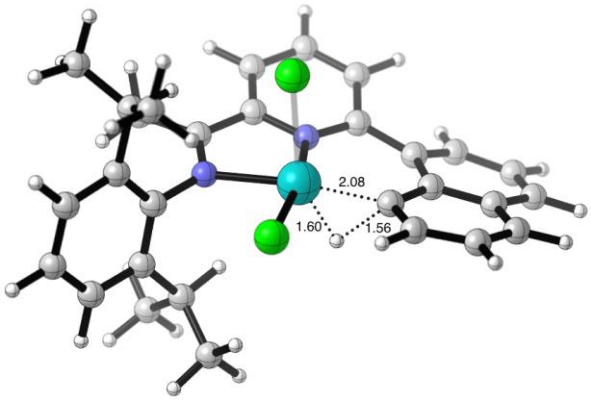

SCF Energy (gas phase) = -2281.17488041
Zero-point correction= 0.500463 (Hartree/Particle)
Thermal correction to Energy = 0.534346
Thermal correction to Enthalpy = 0.535290
Thermal correction to Gibbs Free Energy = 0.435641
Lowest frequency = -761.13cm-1
SCF Energy (AcOH + D3) = -2281.30754055
SCF Energy (PhMe + D3) = -2281.29712525

D:ortho

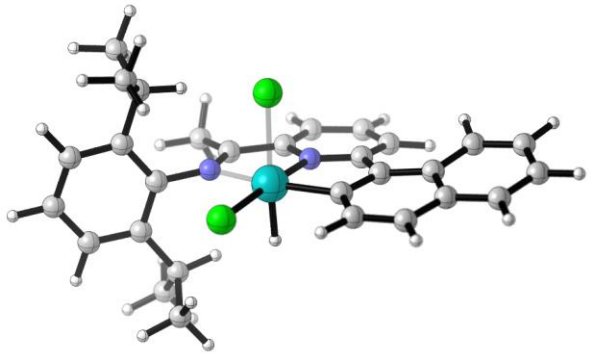

SCF Energy (gas phase) = -2281.19238414
Zero-point correction= 0.502370 (Hartree/Particle)
Thermal correction to Energy = 0.536546
Thermal correction to Enthalpy = 0.537491
Thermal correction to Gibbs Free Energy = 0.436632
SCF Energy (AcOH + D3) = -2281.32091185
SCF Energy (PhMe + D3) = -2281.31093487

D:peri

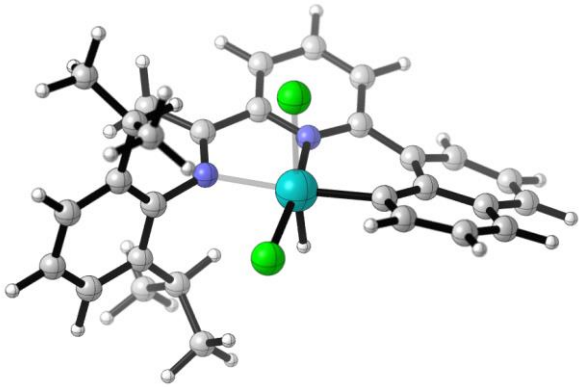

SCF Energy (gas phase) = -2281.18903992
Zero-point correction= 0.502615 (Hartree/Particle)
Thermal correction to Energy = 0.536546
Thermal correction to Enthalpy = 0.537490
Thermal correction to Gibbs Free Energy = 0.438274
SCF Energy (AcOH + D3) = -2281.32084194
SCF Energy (PhMe + D3) = -2281.31121408

HCl

SCF Energy (gas phase) = -460.828400917
Zero-point correction= 0.006554 (Hartree/Particle)
Thermal correction to Energy = 0.008915
Thermal correction to Enthalpy = 0.009859
Thermal correction to Gibbs Free Energy = -0.011345
SCF Energy (AcOH + D3) = -460.83120917
SCF Energy (PhMe + D3) = -460.83009372

References

S1. Gaussian 09 (Revision E.01), M. J. Frisch, G. W. Trucks, H. B. Schlegel, G. E. Scuseria, M. A. Robb, J. R. Cheeseman, G. Scalmani, V. Barone, B. Mennucci, G. A. Petersson, H. Nakatsuji, M. Caricato, X. Li, H. P. Hratchian, A. F. Izmaylov, J. Bloino, G. Zheng, J. L. Sonnenberg, M. Hada, M. Ehara, K. Toyota, R. Fukuda, J. Hasegawa, M. Ishida, T. Nakajima, Y. Honda, O. Kitao, H. Nakai, T. Vreven, J. A. Montgomery, Jr., J. E. Peralta, F. Ogliaro, M. Bearpark, J. J. Heyd, E. Brothers, K. N. Kudin, V. N. Staroverov, T. Keith, R. Kobayashi, J. Normand, K. Raghavachari, A. Rendell, J. C. Burant, S. S. Iyengar, J. Tomasi, M. Cossi, N. Rega, J. M. Millam, M. Klene, J. E. Knox, J. B. Cross, V. Bakken, C. Adamo, J. Jaramillo, R. Gomperts, R. E. Stratmann, O. Yazyev, A. J. Austin, R. Cammi, C. Pomelli, J. W. Ochterski, R. L. Martin, K. Morokuma, V. G. Zakrzewski, G. A. Voth, P. Salvador, J. J. Dannenberg, S. Dapprich, A. D. Daniels, O. Farkas, J. B. Foresman, J. V. Ortiz, J. Cioslowski, and D. J. Fox, Gaussian, Inc., Wallingford CT, 2013.

S2. (a) A.D. Becke, *Phys. Rev. A*, 1988, **38**, 3098; (b) J. P. Perdew, *Phys. Rev. B*, 1986, **33**, 8822-8824.

S3. D. Andrae, U. Haeussermann, M. Dolg, H. Stoll, and H. Preuss, *Theor. Chem. Acc.*, 1990, **77**, 123-124.

S4. (a) W. J. Hehre, R. Ditchfield, and J. A. Pople, *J. Chem. Phys.*, 1972, **56**, 2257; (b) P.C. Hariharan and J. A. Pople, *Theor. Chem. Acta*, 1973, **28**, 213-222.

S5. S. Grimme, J. Antony, S. Ehrlich, and H. Krieg, *J. Chem. Phys*., 2010, **132,** 154104.

S6. J. Tomasi, B. Mennucci, and R. Cammi, *Chem. Rev.*, 2005, **105**, 2999-3093.

S7. See references presented in the main text.